Atomic Compton profile of neon calculated from an accurate Kohn-Sham potential

A. I. Al-Sharif*

Department of Physics, Faculty of Science, Yarmouk University, Irbid, Jordan
(Received 26 October 2004; revised manuscript received 22 February 2005; published 1 July 2005)

The Compton profile of the neon atom is calculated from an accurate Kohn-Sham potential derived from accurate quantum Monte Carlo wave functions. Compared to the experiment, the results are better than the Hartree-Fock ones in the low-wave-vector region. This suggests that the systematic error in the Kohn-Sham formulation in momentum space is relatively small. The first-order Lam-Plazman correction is also calculated. This correction is less than 1% on the average.

I. INTRODUCTION

Wave functions, as established by quantum theory, represent the maximum knowledge we can acquire about a given system. In terms of wave functions all observables, which constitute the link with experiment, can be calculated in principle. Since only a few systems have their exact wave functions known, testing the quality of approximate wave functions is an important field of study. Energy spectrum and position space observables are very common tests. The variational nature of energy computation makes it insensitive to small variations in wave functions and so it cannot be used as a precise measure of the quality of the tested wave functions. In order to overcome this problem, one needs to compute observables that do not share the same eigenfunctions with the Hamiltonian (i.e., do not commute with the Hamiltonian), such as momentum-space observables. Nowadays, experimental work has given direct access to one-electron momentum densities $\omega(\vec{p})$. Hence momentum-space observables can be used to further test approximate wave functions. Among the momentum-space observables, the Compton profile $J(\vec{q})$ has been given much theoretical and experimental attention [1]. Atomic Compton profiles can be obtained [2] by means of photon-photon or photon-electron coincidence measurements, high-resolution Compton scattering, angular correlation of positron annihilation radiation, $(e,2e)$ coincidence spectroscopy, and magnetic Compton scattering experiments. The aim of the present work is to investigate the neon Compton profile calculated within the framework of the Kohn-Sham (KS) formulation of density functional theory (DFT).

DFT as formulated in the two well-known papers by Hohenberg and Kohn [3] and Kohn and Sham [4] is a fundamental quantum theory of matter. It describes successfully the ground state of an interacting electron gas in an external static potential. In the KS formulation of DFT, the problem of N interacting electrons is being transformed to a set of N noninteracting electrons moving in a one-body effective potential called the KS potential V_{ks}. A very important ingredient of the KS potential is the so-called exchange-correlation (XC) potential V_{xc} which is an *ad hoc* medicine invented for

the relief of all the headache caused by the many-body effects. The KS formulation is exact in the position space. Therefore it should give correct results for any observable that depends only on the position coordinates. In momentum space, however, only correct projections on the position space are guaranteed. The KS momentum distribution of the homogeneous electron gas is a clear example. The homogeneous electron gas is simply a system comprising a large number $N \rightarrow \infty$ of electrons moving in a large volume $V \rightarrow \infty$ such as to keep the density finite $n=N/V$. Throughout this volume there should be a uniformly spread out positive charge sufficient to make the whole system neutral. The KS equations under these conditions are satisfied by a single determinant of plane waves. This results in a momentum density which is nothing but a theta function $\omega(p)=2\Theta(p_F - p)$, p_F being the Fermi momentum. This means that all the states with momentum less than, or equal to, the Fermi momentum are occupied and the rest of the momentum states are empty. In the real interacting uniform electron gas, however, electron motion is correlated. Remaining within the single-particle orbitals scheme we can, in principle, describe the ground state of this system by an infinite number of spin orbitals. In contrast to the KS N spin orbitals the occupation number N_i in this case is less than 1 for states under the Fermi momentum and greater than 0 for states above the Fermi momentum. As a perturbationally justified rule of thumb, the respective deviations from 1 and 0 (the KS choice) are larger the closer we are to the Fermi momentum. Now, to what extent can we depend on the KS approach in calculating observables that involve momentum coordinates? Nobody can give a definite answer, since all the known implementations of the KS method are approximate. They involve approximate XC potentials V_{xc}, among which the local density approximation (LDA) is the most common. Recently, access to excellent-quality KS potentials has been achieved [5–8]. They are calculated starting with accurate charge densities derived from quantum Monte Carlo (QMC) many-body wave functions. The algorithm used to generate these potentials starts by expanding V_{xc} in a complete set of basis functions. The expansion coefficients are then varied, solving the KS equations and generating a new charge density each time. This cycle stops when the obtained charge density matches the accurate QMC density. Having these accurate KS potentials in our hands would help us separate the

*Electronic address: alsharif@yu.edu.jo

TABLE I. Occupied orbitals of the neon atom expressed in STO's as in Eq. (5).

j	$c_j(1s)$	$c_j(2s)$	a_j	n_j	$c_j(2p)$	a_j	n_j
1	0.630574	0.038640	10.8072	1	−0.182296	3.7957	2
2	0.387660	0.282352	7.47780	1	0.212390	1.2874	2
3	0.007726	−0.736646	2.59110	2	−0.296368	0.1010	2
4	−0.017984	−0.362927	4.31870	2	1.838318	2.9203	2
5	−0.003771	−0.034733	0.20340	2	−0.830907	3.8012	3
6	0.005506	0.049519	0.11190	2	0.076012	0.2490	3
7	−0.002356	−0.038195	1.33390	3	0.125731	0.1474	3
8	0.001885	0.019742	0.72900	3	0.004876	0.0700	3
9	−0.019841	−0.179849	0.15710	3	0.080557	0.1445	4
10	0.017109	0.155732	0.16860	3	0.038088	0.1163	4

error coming from the approximation for V_{xc} and hence to estimate the momentum distribution error retained to the KS method itself. This would answer the fundamental question of reliability of the KS approach in calculating observables involving momentum coordinates.

The rest of this paper is organized as follows: In Sec. II, theoretical and computational details are presented. In Sec. III, the obtained results are listed and discussed. Finally, the conclusions from this work are drawn in Sec. IV.

II. THEORY AND COMPUTATIONAL DETAILS

At the one-electron level, four observables are the key quantities: the position density $\rho(\vec{r})$ (often unsystematically called the "charge density"), the form factor $F(\vec{k}) = F(\vec{\chi})$ with $\vec{\chi} = \hbar\vec{k}$ of diffraction work, the momentum density $\omega(\vec{p})$, and the reciprocal form factor $B(s)$. In the case of spherical symmetry (atoms, liquids, glasses, powders) and within the impulse approximation, there are particularly simple relationships between the spherically averaged momentum density $\varpi(p)$, the Compton profile $J(q)$ and the reciprocal form factor $B(s)$ [9]:

$$J(q) = \frac{1}{2}\int_{|q|}^{\infty} p\varpi(p)dp = \frac{1}{\pi}\int_{-\infty}^{\infty} B(s)\cos(qs)ds, \quad (1)$$

where $\varpi(p)$ is the spherically averaged momentum density and atomic units are assumed throughout. Equation (1) reveals two methods for the calculation of the Compton profile. Starting from the single-particle eigenfunctions $\{\psi(\vec{r})\}$, which are a natural output of any atomic program, one can calculate the reciprocal form factor $B(s)$,

$$B(s) = \int \rho(\vec{r}, \vec{r}+\vec{s})d\vec{r} = \sum_{i=1}^{N} \int \psi_i(\vec{r})\psi_i(\vec{r}+\vec{s})d\vec{r}, \quad (2)$$

where N is the number of occupied orbitals, then perform the Fourier transform in order to obtain $J(q)$. This involves two-center overlap integrals which are usually hard to evaluate. The other method which is rather simpler is to Fourier transform the eigenfunctions first, then calculate the radial momentum density $\varpi(p)$, and finally obtain the Compton profile via

$$J(q) = \frac{1}{2}\int_{|q|}^{\infty} p\varpi(p)dp. \quad (3)$$

To evaluate the integrals involved in the methods described above, it is common practice to expand the eigenfunctions in a finite basis set.

In the present calculations I started from Umrigar's V_{ks} for neon. This potential enjoys excellent quality as evident from our previous work [10]. The KS eigenfunctions were then calculated directly in terms of Slater-type orbitals (STO's):

$$\phi(r, \vartheta, \varphi; a_j, n_j, l, m) = \frac{(2a_j)^{n_j+1/2}}{\sqrt{(2n_j)!}} r^{n_j-1} e^{-a_j r} Y_{lm}(\vartheta, \varphi), \quad (4)$$

where $Y_{lm}(\vartheta, \varphi)$ are the spherical harmonics and a_j and n_j are optimization parameters. The exponents a_j of these STO's were optimized to get a faithful representation of the KS orbitals $\psi(r, \vartheta, \varphi; n, l, m)$ using a relatively small number of basis functions $\phi(r, \vartheta, \varphi; a_j, n_j, l, m)$—namely, ten orbitals:

$$\psi(r, \vartheta, \varphi; n, l, m) = \sum_{j=1}^{10} c_j \phi(r, \vartheta, \varphi; a_j, n_j, l, m). \quad (5)$$

The optimization algorithm is described elsewhere [11], and the resultant optimized expansions of the occupied orbitals of neon are shown in Table I. Note that the matrix elements of our KS Hamiltonian are m independent. Therefore the listed expansion coefficients $c_j(nl)$ are the same for all m values belonging to a given choice of n and l.

Using Table I, the Compton profile is calculated following both methods described above. As a theoretical benchmark, I also calculated the valence Compton profile using the Roothaan Hartree-Fock (HF) atomic wave functions obtained from the recent tables of Bunge et al. [12].

The final step in the present calculations was to compute the first-order correction to the Compton profile suggested by Lam and Plazman [13] and Bauer [14]. First the correction to the momentum density is found using

TABLE II. Valence Compton profile of the neon atom (the 1*s* orbital contribution is not counted). The first and last columns represent the present calculations using HF and KS wave functions, respectively. The middle ones represent the experimental results from Ag and Mo radiation and the average of them, respectively.

q	HF	Expt. Ag	Expt. Mo	Expt. Av	KS-UMR
0.0	2.548	2.565	2.598	2.582	2.567
0.1	2.540	2.556	2.592	2.574	2.559
0.2	2.515	2.536	2.577	2.558	2.535
0.3	2.475	2.505	2.533	2.519	2.492
0.4	2.418	2.438	2.465	2.451	2.431
0.5	2.335	2.350	2.369	2.359	2.349
0.6	2.236	2.243	2.255	2.249	2.245
0.7	2.120	2.122	2.126	2.124	2.123
0.8	1.990	1.988	1.984	1.986	1.990
0.9	1.855	1.842	1.836	1.839	1.849
1.0	1.715	1.690	1.679	1.685	1.706
1.2	1.435	1.398	1.390	1.394	1.426
1.4	1.171	1.134	1.145	1.140	1.171
1.6	0.953	0.912	0.930	0.921	0.948
1.8	0.766	0.744	0.754	0.749	0.762
2.0	0.619	0.611	0.605	0.608	0.609
2.5	0.355	0.366	0.347	0.355	0.351
3.0	0.212	0.228	0.222	0.225	0.209
3.5	0.132	0.154	0.158	0.156	0.131
4.0	0.085	0.094	0.111	0.102	0.086
5.0	0.040	0.047	0.036	0.041	0.041

$$\delta\varpi(p) = \int_0^\infty [N(p;\rho(r)) - N_{ks}(p;\rho(r))]\rho(r)dr, \qquad (6)$$

where $N(p;\rho(r))$ is the momentum density of the nonpolarized homogeneous interacting electron gas and $N_{ks}(p;\rho(r))$ is the momentum density of the noninteracting electron gas (the Fermi distribution function). The subscript *ks* indicates the fact that this is the momentum distribution obtained from KS calculations for the interacting case. $N(p;\rho(r))$ is obtained from Monte Carlo simulations by Senatore *et al.* [15]. The result of Eq. (6) is then inserted into Eq. (3) to get the Lam-Plazman (LP) correction to the Compton profile.

III. RESULTS AND DISCUSSION

An experimental Compton profile of atomic neon is reported in the work by Eisenberger [16], where an accurate experimental procedure was followed incorporating corrections to the impulse approximation. Two radiation sources—namely, Ag and Mo—have been used and the resultant Compton profiles were compared with theoretical calculations referenced as "personal communication." Another investigation of the neon Compton profile with a comparison between theory and experiment has also been performed [17,18] where, in the latter, the calculations were performed

within the KS framework using the LDA and self-interaction corrected (SIC) LDA.

The results of the present calculations are summarized in Table II. In this table, the contribution from the 1*s* orbital was ignored. This has to do with problems related to the impulse approximation since the 1*s* orbital lies in the core region where the electrons are tightly bound to the nucleus. The first and last columns represent the present calculations using the HF and KS wave functions respectively. The middle ones represent the experimental results obtained us-
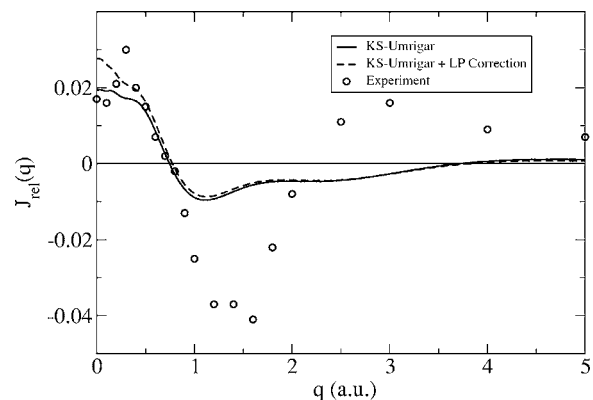
FIG. 1. The KS and experimental valence Compton profiles relative to the HF one plotted from Table II. The experimental profile is obtained using the Ag radiation source.

TABLE III. Compton profile of the neon atom. The first column represents the Compton profile generated from Umrigar's potential. The middle ones are theoretical calculations from Ref. [18]. The last column contains experimental results reported by the same reference.

q	KS-UMR	KS-LDA	KS-SIC	Expt.
0.0	2.741	2.806	2.702	2.762
0.1	2.733	2.797	2.695	2.754
0.2	2.708	2.770	2.670	2.738
0.3	2.665	2.723	2.627	2.698
0.4	2.604	2.653	2.567	2.630
0.5	2.521	2.559	2.486	2.537
0.6	2.416	2.444	2.386	2.427
0.7	2.294	2.312	2.272	2.301
0.8	2.159	2.167	2.145	2.162
0.9	2.018	2.016	2.009	2.014
1.0	1.874	1.863	1.869	1.859
1.2	1.591	1.569	1.593	1.565
1.4	1.332	1.306	1.338	1.308
1.6	1.106	1.083	1.115	1.086
1.8	0.916	0.899	0.929	0.910
2.0	0.760	0.749	0.776	0.765
2.5	0.490	0.493	0.511	0.501
3.0	0.337	0.344	0.355	0.359
3.5	0.246	0.254	0.261	0.277
4.0	0.188	0.195	0.200	0.210
5.0	0.119	0.125	0.127	0.126
6.0	0.079	0.085	0.087	-
7.0	0.053	0.059	0.061	-
8.0	0.036	0.042	0.043	-
9.0	0.026	0.030	0.031	-
10.0	0.015	0.022	0.022	-

FIG. 2. The KS and experimental Compton profiles of the Ne atom plotted from Table III. Different KS implementations are shown. The Compton profile generated from Umrigar's potential is represented by a solid line.

To compare with the KS Compton profiles reported by Sawant and Kanhere [18], I repeated the calculations including the $1s$ orbital contribution. Again, in the small q values, the results obtained from the Umrigar-KS potential are close to the experiment as expected. The results are summarized in Table III and plotted in Fig. 2. In this figure, the Compton profiles for only small q values were plotted since this is the only part where the differences between them is noticeable. As seen in this figure, the experimental profile lies between the LDA and Umrigar's profiles. It is surprising to see that the LDA profile is closer to the experimental profile than the SIC one although it is known that the SIC KS potential is better than the LDA one. In fact, the SIC potential enjoys the $1/r$ asymptote while the LDA one does not. The authors attributed this discrepancy to numerical inaccuracies in calculating the Fourier transform of the wave functions having a long tail.

ing the Ag source, the Mo source, and the average of these two results, respectively. We can see clearly in Table II that the KS results are better than the HF results in the small-q range.

One thing that merits mention is the fact that the Mo experiment suffers greatly from the impulse approximation [16]. If we consider only the Ag experiment as already done by some authors [17], then we see an excellent agreement with the experiment. In order to have a more clear vision of this agreement, I plotted in Fig. 1 the experimental Compton profile obtained using the Ag source and the KS profile, both relative to the HF one (the HF Compton profile is subtracted). The noted inability of the HF profile (represented by a straight line in the figure) to follow the experimental one, especially in the low-q region, is understood on the basis of the lack of many-body correlations in the HF wave functions. In the same figure, the LP-corrected version of the KS Compton profile is also shown. The LP correction due to Eq. (6) is of the order of 0.005 on the average which is less than 1%. The correction dies away quickly along the q axis. In fact, the LP correction to the momentum density is only significant in the vicinity of $q=0$.

IV. CONCLUSION

In this work, the Compton profile of atomic Ne is calculated starting with a very accurate KS potential. The resultant profile agrees very well with the experimental one especially in the low-q region. In order to assess what such an agreement really means, the HF Compton profile is computed. The HF profile is actually the best exchange-only profile that can be ever obtained. Nevertheless, the role of the many-body correlations, which is completely missing in the HF scheme, is found to be significant to the limit of pushing the HF profile relatively away from the experimental one. The LP correction to the Compton profile is also computed. This correction dies away quickly along the q axis. In fact, the LP correction is very small and noticeable only in the vicinity of $q=0$. Those results show that, despite the known systematic error in the KS formulation of the DFT in momentum space, it is still reliable to calculate observables involving the momentum coordinates. Corrections do not represent a computational difficulty and can be easily performed. In any case, corrections have a relatively small contribution.

[1] B. Williams, *Compton Scattering: The Investigation of Electron Momentum Distributions*, (McGrawHill, New York, 1977).

[2] J. C. Angulo, J. Antolin, and A. Zarzo, Z. Phys. D: At., Mol. Clusters **28**, 269 (1993).

[3] P. Hohenberg and W. Kohn, Phys. Rev. **136**, B864 (1964).

[4] W. Kohn and L. J. Sham, Phys. Rev. **140**, A1133 (1965).

[5] C. J. Umrigar and X. Gonze, in *High Performance Computing and its Application to the Physical Sciences, proceedings of the Mardi Gras '93 Conference*, edited by D. A. Browne *et al.* (World Scientific, Singapore, 1993).

[6] C. J. Umrigar and X. Gonze, Phys. Rev. A **50**, 3827 (1994).

[7] C. J. Umrigar and X. Gonze (unpublished).

[8] See, e.g., R. C. Morrison and Q. Zhao, Phys. Rev. A **51**, 1980 (1995);E. J. Baerends, O. V. Gritsenko, and R. van Leeuwen, in *Chemical Applications of DFT*, edited by B. B. Laird, R. B. Ross, and T. Ziegler, Am. Chem. Soc. Symp. Ser. No. 629 (American Chemical Society, Washington, DC, 1996).

[9] Wolf Weyrich, in *Quantum-Mechanical Ab-initio Calculation of the Properties of Crystalline Materials*, edited by Cesare Pisani editor (Springer-Verlag, Berlin, 1996).

[10] A. I. Al-Sharif, R. Resta, and C. J. Umrigar, Phys. Rev. A **57**, 2466 (1998).

[11] A. I. Al-Sharif (unpublished).

[12] C. F. Bunge, J. Barriesntos, and A. V. Bunge, At. Data Nucl. Data Tables **53**, 113 (1993).

[13] L. Lam and P. M. Plazman, Phys. Rev. B **9**, 5122 (1974).

[14] Gerrit E. W. Bauer, Phys. Rev. B **27**, 5912 (1983).

[15] G. Senatore, S. Moroni, and D. M. Ceperly, in *Physics of Strongly Coupled Plasmas*, edited by W. D. Kraeft and M. Schlanges (World Scientific, Singapore, 1996), p. 429.

[16] P. Eisenberger, Phys. Rev. A **5**, 628 (1972).

[17] H. Schmider, V. H. Smith, and Wolf Weyrich, Z. Naturforsch., A: Phys. Sci. **48**, 221 (1993).

[18] V. R. Sawant and D. G. Kanhere, J. Phys. B **17**, 3003 (1984).